accepted by Physical Review B, 2002

Dynamical bistability in quantum dot structures: The role of Auger processes

A. Rack, R. Wetzler, A. Wacker, and E. Schöll
Institut für Theoretische Physik, Technische Universität Berlin, Hardenbergstr. 36, 10623 Berlin, Germany
(Dated: February 1, 2008)

Bistability in quantum dot structures is examined by a drift-diffusion model in combination with electron capture and emission processes. Our simulations provide a dynamic scenario with extremely long switching times of the order of months and the results are in good agreement with the experimental findings of Yusa and Sakaki [Appl. Phys. Lett. **70**, 345 (1997)]. The analysis of the data supports the importance of Auger capture processes for quantum dots.

PACS numbers: 73.63.Kv,85.35.Be

arXiv:cond-mat/0207099v2 [cond-mat.mes-hall] 10 Sep 2002

I. INTRODUCTION

Semiconductor quantum dots (QDs) formed by self-organized growth processes [1] allow for the spatial confinement of electrons on a scale of 10 nm. This suggests that these structures may serve as extremely small memory devices. A first step in this direction is the investigation of specially grown structures where the charging of a layer of QDs could be detected via its influence on the conductivity of a two dimensional electron gas [2, 3]. These experiments showed a pronounced bistability (up to room temperature [4]) depending on the history of the bias sweep. The sensitivity to light illumination suggests a variety of applications in photoelectronic devices [5, 6].

A key issue towards a detailed understanding of these experiments is the question if the observed bistability is of transient nature, and the order of the time scales involved. In order to elucidate this point we performed a simulation of the experiment from Ref. 2 applying a drift-diffusion model combined with the generation-recombination (GR) kinetics of the QDs. Our results show that the experiments can be well described if Auger processes constitute the dominant GR-processes. Therefore this type of experiments may serve as an additional tool to shed light into the controversial issue on the nature of electron capture in quantum dots [7, 8, 9].

II. THE MODEL

Here we consider the structure used in the experiment of Ref. 2 as sketched in Fig. 1. From the experimentally determined size of the QDs (height $h = 5$ nm and diameter 20 nm) we estimate a ground state binding energy of $E_\mathrm{b} = 250$ meV [10]. We use a QD density $N_\mathrm{QD} = 7.5 \times 10^{10}/\mathrm{cm}^2$.

We model the transport in the conduction band by a drift-diffusion approach assuming a stationary state similar to Ref. 11, which is justified if the dielectric relaxation time is short compared to other dynamical features. This provides us with the one-dimensional continuity equation

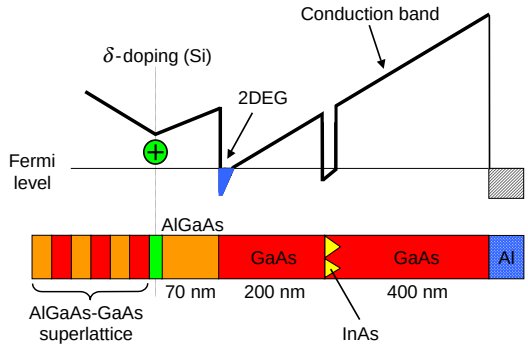

FIG. 1: Sketch of the sample used in Ref. 2 together with the resulting conduction band profile at zero bias.

$$-\frac{\partial}{\partial z}\left[\mu n(z)\frac{\partial}{\partial z}E_F(z)\right] = ef[n(z_\mathrm{QD}), n^\mathrm{2D}_\mathrm{QD}(t)]\chi_\mathrm{QD}(z) \tag{1}$$

with the characteristic function

$$\chi_\mathrm{QD}(z) := \begin{cases} 1/h & (z \in \text{QD layer}) \\ 0 & (z \notin \text{QD layer}) \end{cases} \tag{2}$$

and the electron capture rate f which determines the electron density in the QD layer (in units $\mathrm{sec}^{-1}\mathrm{cm}^{-2}$)

$$\frac{\partial}{\partial t} n^\mathrm{2D}_\mathrm{QD}(t) = f[n(z_\mathrm{QD}), n^\mathrm{2D}_\mathrm{QD}(t)]\,. \tag{3}$$

Here, $e > 0$ is the elementary charge, $\mu = 2\times 10^5\ \mathrm{cm}^2/\mathrm{Vs}$ is the electron mobility (at 77 K) and $n^\mathrm{2D}_\mathrm{QD}$ is the density per unit area of the electrons trapped within the QDs at position z_{QD}, E_F is the Quasi-Fermi level of the electrons, which is related to the free electron density n by

$$\begin{aligned} n(z) &= N_c(z) F_{1/2}\left(\frac{E_F(z) - E_{c0}(z) + e\phi(z)}{k_B T}\right) \\ \text{with} \quad N_c &= 2\left(\frac{m_e k_B T}{2\pi\hbar^2}\right)^{3/2} \end{aligned} \tag{4}$$

and the Fermi integral $F_{1/2}$. Here m_e is the effective mass, E_{c0} the intrinsic band edge of the conduction band

(we set $E_{c0} = 0$ for GaAs and use $E_{c0} = 0.198$ meV for the $Al_{0.25}Ga_{0.75}As$ layer), T the lattice temperature, k_B Boltzmann's constant, and ϕ denotes the electric potential. Quantization effects in the two dimensional electron gas are neglected for simplicity.

The electron capture rate f is assumed to be a combination of Auger processes and single electron processes (like multi-phonon capture and emission) in the following way:

$$f[n(z_{\rm QD}), n_{\rm QD}^{\rm 2D}] = (Cn^{\rm 2D} + \sigma)(n^{\rm 2D} p_{\rm QD}^{\rm 2D} - n_1^{\rm 2D} n_{\rm QD}^{\rm 2D}) \quad (5)$$

Here $n^{\rm 2D} = n(z_{\rm QD})h$ is the effective free electron density at the QDs per unit area (which may be related to a wetting layer density of the same order of magnitude), $p_{\rm QD}^{\rm 2D} = 2N_{\rm QD} - n_{\rm QD}^{\rm 2D}$ is the density of unoccupied QD states for twofold degeneracy. C and σ are the rate coefficients for the Auger and multi-phonon process, respectively (see also Ref. 8). For the Auger process, electron capture requires the presence of two electrons in the vicinity of the QD, as well as an empty dot state. Thus the capture rate is proportional to $(n^{\rm 2D})^2 p_{\rm QD}^{\rm 2D}$. In contrast, for single electron processes the energy is transfered to different degrees of freedom (such as phonons) and the rate is proportional to $n^{\rm 2D} p_{\rm QD}^{\rm 2D}$. The respective electron emission rates (with negative sign) are obtained from the principle of detailed balance for equilibrium distributions [12]. Assuming nondegeneracy in the conduction band, we find $n^{\rm 2D} = N_c h \exp[(E_F + e\phi)/k_B T]$ and $n_{\rm QD}^{\rm 2D}/p_{\rm QD}^{\rm 2D} = \exp[(E_F + E_b + e\phi)/k_B T]$ in equilibrium. Thus $n^{\rm 2D} p_{\rm QD}^{\rm 2D}/n_{\rm QD}^{\rm 2D} = N_c h \exp(-E_b/k_B T) \equiv n_1^{\rm 2D}$, and the prefactor $n_1^{\rm 2D}$ in Eq. (5) ensures the vanishing of the rates in thermodynamic equilibrium.

The continuity equation (1) has to be combined with the one-dimensional Poisson equation

$$\begin{aligned} -\epsilon_0 \frac{\partial}{\partial z}\left[\epsilon_r(z)\frac{\partial}{\partial z}\phi(z)\right] &= \rho(z) \\ \text{with} \quad \rho(z) &= e[N_D^+(z) - n(z) - n_{\rm QD}^{\rm 2d}(t)\chi_{\rm QD}(z)] \end{aligned} \quad (6)$$

where N_D^+ is the density of ionized donors resulting from the δ-doping and ϵ_0 and ϵ_r are the absolute and relative permittivity.

The boundary condition for the quasi-Fermi level is $E_F = 0$ at the AlGaAs/GaAs interface due the contact with the two dimensional electron gas (2DEG) and $E_F = -eV_g$ at the GaAs/Al interface. Here the Schottky barrier height $E_S = 1.0$ eV determines the difference between the conduction band edge and the Fermi level in the metal. Thus $-e\phi(z_{\rm Schottky}) = E_S - eV_g$ provides a Dirichlet boundary condition for ϕ. The second boundary condition of Neumann type results from the charge of the ionized donors at the δ-doping. All calculations are performed at 77 K.

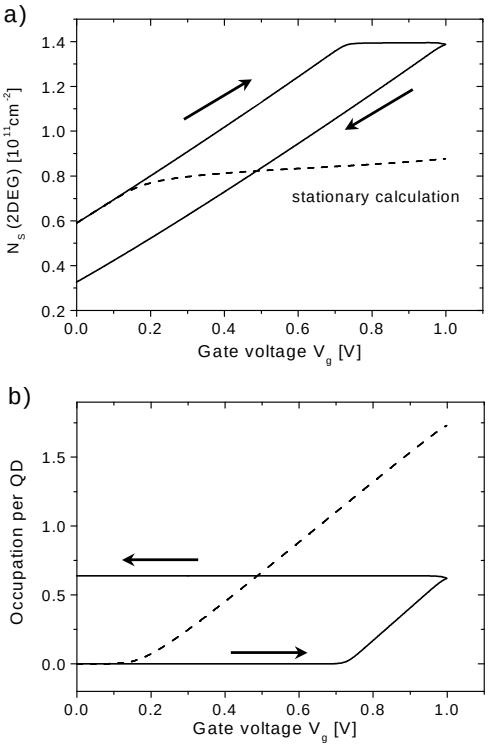

FIG. 2: (a) Channel electron density N_s versus bias V_g applied to the gate contact for a bias sweep. The duration of the entire sweep is one hour and an Auger coefficient $C = 2 \times 10^{-12}$ cm$^4/s$ is used. (b) corresponding occupation probability of the QDs.

III. RESULTS

At first we consider only Auger processes. We use $C = 2 \times 10^{-12}$ cm$^4/s$, which was calculated in Ref. 13. Fig. 2(a) shows the density N_s of the 2DEG versus the gate voltage for a bias sweep from $V_g = 0$ V to 1 V and back to 0 V (indicated by the arrows) with a constant sweep rate and a total sweep duration of 1 hour [14]. The findings are in excellent agreement with the corresponding experimental data, see the broken line of Fig. 1 in Ref. 2, except for an overall shift of the densities by $\sim 2 \times 10^{10}$/cm^2 (larger density in the experiment). Fig. 2(b) shows the corresponding occupation probability of the QDs, demonstrating that the charging state of the QDs discriminates between the different conducting states. For a comparison we have also shown the result for the stationary situation $f[n, n_{\rm QD}^{\rm 2D}] = 0$. This shows that both during the up- and down-sweep nonequilibrium distributions persist, as the GR rates are not fast enough to establish thermodynamic equilibrium.

The dynamical nature of the bistability manifests itself in the time dependence of the bias sweep, see Fig. 3. This shows that the behavior is robust against changes in the time scales by several orders of magnitude albeit the plateau density where the dots are charged is slightly

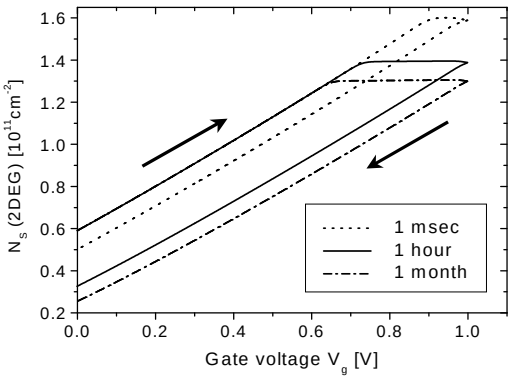

FIG. 3: N_s-V_g-characteristic calculated for different sweep durations. An Auger coefficient $C = 2 \times 10^{-12}$ cm$^4/s$ is used.

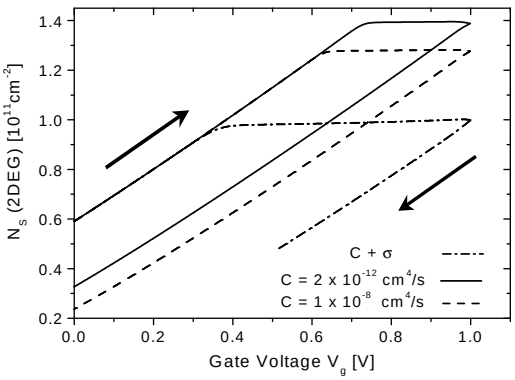

FIG. 4: N_s-V_g-characteristic calculated with different values of the coefficient C with $\sigma = 0$ (full and dashed line) as well as $C = 10^{-8}$cm$^4/s$ and $\sigma = 1$cm$^2/s$ (dash-dotted line). The entire sweep duration is one hour.

changing with the sweep duration. Below this density the charge on the QDs is hardly changed even for the slowest sweep rate. This result indicates that the branches are stable on rather long time scales, an important feature for possible applications. Time scales of 100 h have been demonstrated in Ref. [4] at room temperature where a more complicated structure was used.

The rather long relaxation times are due to the fact that Auger rates depend quadratically on the electron density n, see Eq. (5). Indeed the potential profile provides rather low electron densities at the QDs for biases below $\approx 0.7V$, leading to a very small capture rate.

The $N_s(V_g)$ characteristic can be understood as follows: Starting from equilibrium at $V_g = 0$, the quantum dots are essentially unoccupied. This implies a linear potential distribution over the entire GaAs layer with a potential $\phi(z_{\rm QD}) \approx (V_g - E_S/e)W/L$ at the QDs. Here L is the distance between the 2DEG and the Schottky contact and W is the distance between the 2DEG and the QDs. (We used $e\phi(z_{\rm 2DEG}) \approx 0$ as the Fermi level $E_F = 0$ is close to the band edge at the 2DEG.) Assuming that the electrons are in equilibrium with the 2DEG, we have

$$n(z_{\rm QD}) \approx N_c \exp\left(-\frac{E_S - eV_g}{k_B T}\frac{W}{L}\right). \qquad (7)$$

For biases below $V_{\rm crit}$ this density is so small that the corresponding capture rates hardly change the occupation of the QDs on the time scale of the bias sweep. Therefore the linear potential drop in the GaAs layer persists and the density of the 2DEG increases with V_g. At $V_g = V_{\rm crit}$ the capture rate becomes

$$f[n(z_{\rm QD}), 0] = \frac{\partial}{\partial t} n^{\rm 2D}_{\rm QD}(t) = \frac{\epsilon_r \epsilon_0}{e(L-W)}\frac{{\rm d}V_g}{{\rm d}t}. \qquad (8)$$

Then the charge captured in the quantum dots just screens any further increase of the bias, so that the field on the left side of the dots (as well as the density of the 2DEG) remains constant. Sweeping down the bias, the electron density $n(z_{\rm QD})$ decreases and so do the capture rates. Therefore the charge in the QDs remains almost constant during the down sweep, explaining the linear decrease of the 2DEG electron density.

The magnitude of the Auger coefficient is controversial. E.g., in Ref. 8 a value of $C = 10^{-8}$cm$^4/s$ was deduced from experimental data. The corresponding $N_s(V_g)$ curve is given in Fig. 4 (dashed curve). The result differs only slightly but agrees less well with the experimental data. This indicates that the findings are not very sensitive to the magnitude of C which just rescales the time scales. [This follows directly from Eq. (8): Only the ratio between the capture coefficients and ${\rm d}V_g/{\rm d}t$ matters.] The analysis of Ref. 8 provides additionally a single electron capture coefficient $\sigma = 1\,$cm^2/s in Eq. (5). The corresponding result is shown by the dash-dotted line in Fig. 4. The presence of the single electron term strongly changes the behavior. Regarding the large plateau width and its low electron density, this result is not compatible with the experiment [2].

In Fig. (5) the result is given for different single electron capture coefficients σ while Auger processes are neglected (i.e. $C = 0$). Good agreement with the experiment is found for $\sigma = 2 \times 10^{-8}$cm^2/s while values above $\sigma \sim 10^{-4}$cm^2/s are in strong disagreement with the experimental findings.

Experimentally, electron capture times of the order of $10 - 100$ ps for high carrier densities have been observed, see, e.g. Ref. [7] and references cited therein. For dot densities of $10^{10} - 10^{11}$/cm^2 this implies $\sigma \gg 10^{-2}$cm^2/s if single electron processes are dominating. From our study of the dynamical bistability this seems to be too large. On the other hand the Auger coefficient $C = 2 \times 10^{-12}$cm^4/s gives capture times of 25 ps for a (wetting) layer density of 10^{11}/cm^2 and a dot density of 10^{11}/cm^2. The times become even shorter for larger values of $C < 10^{-8}$cm^4/s, which are also consistent with our study.

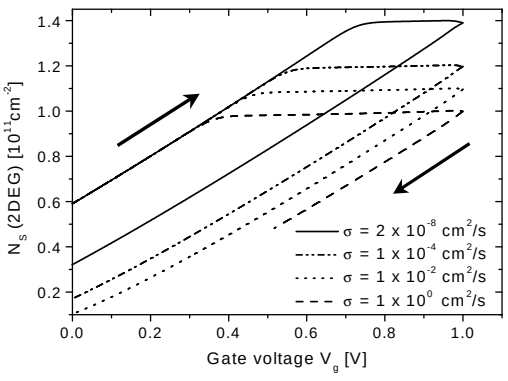

FIG. 5: N_s-V_g-characteristic calculated with different values for the coefficient σ and $C = 0$. The duration of the entire sweep is one hour.

IV. CONCLUSION

We have shown that the bistability observed in quantum dot structures is of dynamical nature with time scales of the order of months under appropriate conditions. The long time scales result from the dependence of the Auger capture and emission rate on the conduction band electron densities. For not too large gate biases, the densities are low and thus the kinetics is extremely slow. The analysis of this kind of experiments allows for additional information to study the relevance of Auger capture in comparison to single electron processes as multiphonon emission. Our findings suggest an upper bound for single electron processes $\sigma < 10^{-4}\mathrm{cm}^2/\mathrm{s}$. Such values are not compatible with observed capture rates at high electron densities. In contrast, Auger capture coefficients in the range of $10^{-12}\mathrm{cm}^4/\mathrm{s} < C < 10^{-8}\mathrm{cm}^4/\mathrm{s}$ agree well with the fast dynamics for high carrier densities and explain the slow dynamics for low carrier densities where the dynamical bistability is observed.

This work was supported by DFG in the framework of SFB 296.

[1] D. Bimberg, M. Grundmann, and N. Ledentsov, *Quantum Dot Heterostructures* (John Wiley & Sons Ltd., New York, 1999).
[2] G. Yusa and H. Sakaki, Appl. Phys. Lett. **70**, 345 (1997).
[3] J. J. Finley, M. Skalitz, M. Arzberger, A. Zrenner, G. Böhm, and G. Abstreiter, Appl. Phys. Lett. **73**, 2618 (1998).
[4] K. Koike, S. Saitoh, S. Li, S. Sasa, M. Inoue, and Y. Yano, Appl. Phys. Lett. **76**, 1464 (2000).
[5] M. C. Bödefeld, R. J. Warburton, K. Karrai, J. P. Kotthaus, G. Medeiros-Ribeiro, and P. M. Petroff, Appl. Phys. Lett. **74**, 1839 (1999).
[6] A. J. Shields, M. P. O'Sullivan, I. Farrer, D. A. Ritchie, K. Cooper, C. L. Foden, and M. Pepper, Appl. Phys. Lett. **74**, 735 (1999).
[7] J. Feldmann, S. T. Cundiff, M. Arzberger, G. Böhm, and G. Abstreiter, J. Appl. Phys. **89**, 1180 (2001).
[8] S. Raymond, K. Hinzer, S. Fafard, and J. L. Merz, Phys. Rev. B **61**, 16331 (2000).
[9] R. Heitz, M. Veit, N. N. Ledentsov, A. Hoffmann, D. Bimberg, V. M. Ustinov, P. S. Kop'ev, and Z. I. Alferov, Phys. Rev. B **56**, 10435 (1997).
[10] O. Stier, M. Grundmann, and D. Bimberg, Phys. Rev. B **59**, 5688 (1999).
[11] R. Wetzler, C. M. A. Kapteyn, R. Heitz, A. Wacker, E. Schöll, and D. Bimberg, Appl. Phys. Lett. **77**, 1671 (2000).
[12] E. Schöll, *Nonequilibrium Phase Transitions in Semiconductors* (Springer, Berlin, 1987).
[13] A. V. Uskov, J. McInerney, F. Adler, H. Schweizer, and M. H. Pilkuhn, Appl. Phys. Lett. **72**, 58 (1998).
[14] G. Yusa (2002), private communication.